INTBECM International Bulletin of Electrochemical Methodology

Fabrication and characterization of a cost-effective electrochemical modified electrode for paracetamol determination in pharmaceutical infusion solution

Alev Yıldırım[a], Demet Uzun[b]*

[a]; *Gazi University Graduate School of Natural and Applied Sciences, Gazi University Central Campus, Ankara, Turkey*

ORCID: 0009-0009-6822-3298

[b]; *Gazi University, Faculty of Science, Department of Chemistry, Ankara, Turkey*

ORCID: 0000-0002-7090-6516

ABSTRACT

Paracetamol (PAR) is a pharmaceutical active ingredient widely used for analgesic and antipyretic purposes. In this study, for the electrochemical determination of PAR, 4-amino-5-(4-pyridyl)-4H-1,2,4-triazole-3-thiol (4P3T) compound was modified on a glassy carbon electrode (GCE) to prepare an electrochemical sensor (4P3T-GCE). The characterization of the modified electrode was carried out using Fourier transform infrared spectroscopy (FTIR), cyclic voltammetry (CV), and electrochemical impedance spectroscopy (EIS) techniques. The prepared and characterized sensor was used in the electrochemical determination of PAR. Electrochemical oxidation and quantitative determination of PAR were performed using the differential pulse voltammetry (DPV) method. PAR determination was successfully carried out in pharmaceutical infusion solution samples using 4P3T-GCE by the standard addition method. The fabricated sensor showed two linear working ranges: 0.55–100 µM and 100–785 µM. The limit of detection (LOD; 3s/m) value was found to be 0.16 µM, and the limit of quantification (LOQ; 10s/m) value was found to be 0.53 µM. The obtained results reveal that the modified electrode is an effective electrochemical sensor for the determination of PAR in pharmaceutical samples due to its features such as high sensitivity, wide linear range, and low LOD.

KEYWORDS

Glassy carbon electrode, paracetamol, pharmaceutical infusion solution, voltammetry

1. INTRODUCTION

In recent years, the unconscious use of pharmaceuticals has become detrimental in terms of developing immunity to the active ingredients in them [1]. Therefore, analysing them plays an important role in providing drug qualification control and protecting human health. Paracetamol (N-acetyl-p-aminophenol, PAR), the subject of this study, is a frequently preferred antipyretic and analgesic drug. It can be sold without a prescription and is frequently consumed in daily life to relieve pain caused by disorders such as muscle pain, toothache, and headache. It can cause toxic effects, especially in cases of

incorrect use. Loss of appetite, diarrhea, vomiting, and liver failure are the main adverse effects [2]. In healthy adults, PAR is metabolised by the liver and excreted in the urine [3]. Only 1–4% is excreted as PAR, and the majority is excreted as PAR glucuronide (47–60%) and PAR sulfate (25–35%). In some cases, oxidation occurs in the P450 system of cytochrome, and a substance is formed named N-acetyl-p-benzoquinone-imine (NAPQI), which exhibits toxic properties. For alcoholics or malnourished patients, higher doses of PAR may lead to an active oxidative pathway, leading to liver necrosis. Therefore, the quantitative determination of PAR is of great importance in various fields, including drug production, analysis of biological samples, environmental analysis, and forensic toxicology [4-6]. Difficulties in PAR determination include co-existing active substances, impurities, interference from metabolites, or degradation products, emphasizing the necessity for sensitive, selective, and cost-effective methods for the PAR determination in biological and pharmaceutical environments [7-9].

Various analytical methods have been developed to determine PAR today. These methods include techniques such as spectrophotometry, chemiluminescence, chromatography, electroanalytical methods (voltammetry, potentiometry), and capillary electrophoresis [10-15]. However, most of these methods are generally associated with lengthy processing steps, high costs, and complex sample preparation. Therefore, other methods can be preferred as an alternative to the mentioned methods. The method to be selected is determined depending on the chemical structure of the substance to be analyzed, its sensitivity, the sample matrix, and the analysis speed.

The use of voltammetric methods for PAR determination has become increasingly widespread in recent years. Voltammetry stands out due to its advantages, including low equipment requirements, short analysis times, high sensitivity, and selectivity. This method, which is particularly suitable for analyzing electroactive substances, is an effective technique for determining the amount of PAR in pharmaceutical preparations and biological samples. In voltammetric studies, the use of modified electrodes for determining target species at low concentrations has become widespread in recent years. Modified electrodes are prepared by coating molecules with functional groups onto the surface of a solid electrode. Among the molecules mentioned, triazoles and their derivatives are frequently used in surface coating applications. These molecules generally

polymerize on the electrode surface and form conductive films. Since these films contain triazole rings and nitrogen atoms, they are sensitive to biological species through non-covalent interactions.

In this study, the 4-amino-5-(4-pyridyl)-thiol (4P3T) compound, which contains triazole and thiol rings in its structure and can therefore easily bind to the electrode surface, was modified on a glassy carbon electrode (GCE), resulting in the production of an electrochemical sensor (4P3T-GCE) was produced. The electrochemical sensor produced was characterized using electrochemical and spectroscopic techniques to demonstrate that the 4P3T compound was successfully coated on the electrode surface. Using the produced sensor, suitable working conditions for the electrochemical determination of PAR were investigated. For this purpose, various supporting electrolytes and pH values were experimented with to determine their effects on the PAR oxidation of 4P3T-GCE. CV was used to perform the scan rate study, resulting in 4P3T-GCE having a high conductivity due to its large surface area. In the calibration study performed using the DPV method under optimum operating conditions, linear working range, LOD, and LOQ for PAR were found, and the standard addition method was used to determine PAR in a pharmaceutical infusion solution.

2. EXPERIMENTAL

2.1. Reagents

4P3T, H_3PO_4 (phosphoric acid, 85%), KCl (potassium chloride), and $HClO_4$ (perchloric acid, 70%) were provided by Sigma-Aldrich (Germany). PAR, NaAc (sodium acetate), H_2SO_4 (sulphuric acid, 97%), NaOH (sodium hydroxide), $K_4[Fe(CN)_6]$ (potassium ferrocyanide), ACN (acetonitrile, HPLC), HAc (acetic acid, glacial), Na_2HPO_4 (disodium hydrogen phosphate), $K_3[Fe(CN)_6]$ (potassium ferricyanide), NaH_2PO_4 (sodium dihydrogen phosphate), H_3BO_3 (boric acid), ferrocene, and TBATFB (tetrabutylammonium tetrafluoroborate) were supplied by Merck (Germany). 0.1 M H_2SO_4 was used to prepare 1 mM 4P3T solution. The stock PAR solution (1 mM) was prepared daily in ultra-pure water. All solvents and reagents were analytical reagent grade. Ferrocene solution was prepared in ACN containing 0.1 M TBATFB as the anhydrous medium. Ultra-pure water was used to prepare the other solutions.

A stock phosphate buffer solution (PBS) was prepared by Na_2HPO_4 and NaH_2PO_4 to achieve a final concentration of 0.1 M.

1.0 M NaOH and/or HCl were used to adjust the pH to different values.

2.2. Apparatus

A CHI 660B electrochemical workstation (CH Instruments, China) containing a three-electrode system was used for the electrochemical studies (CV, DPV, and EIS). For this system, as the working electrode, a bare and covered GCE (BASi, MF-2012, USA), as the aqueous reference electrode, an Ag/AgCl/KCl (sat.) (silver/silver chloride, BASi, MW-2021, USA), and as the counter electrode, a Pt wire (platinum, BASi, MW-1032, USA) were used. Additionally, $Ag/AgNO_3$ (silver/silver nitrate, BASi, MF-2062, USA) was used as the non-aqueous reference electrode. The anhydrous medium containing 0.01 M Ag^+ was used to prepare this electrode. All experimental measurements were carried out at room temperature.

A Thermo Fisher Scientific brand spectrophotometer (Nicolet IS5 model, US) was used to obtain FT-IR spectra. It contains an ATR with a diamond lens and a KBr pellet head.

2.3. The coating process of the GCE surface

The uncoated GCE surfaces were polished on the microcloth pad with 0.3 and 0.05 µm alumina slurry. After that, the following operations were carried out in order: The electrodes were rinsed with ultra-pure water, sonicated in ACN and ultra-pure water for 10 min, and dried in air. The cleaned and dried GCE was immersed in a 1 mM 4P3T solution prepared in 0.1 M H_2SO_4. The CV was taken at a scan rate of 100 mV s^{-1} between −1.2 V and +2.0 V for 10 cycles. Thus, the prepared electrode (4P3T-GCE) was rinsed again with ultra-pure water to remove any physically adsorbed monomer species.

2.4. Electrochemical determination using DPV

PAR was determined with the 4P3T-GCE in 0.1 M pH 4.5 PBS buffer using DPV at 25±1 °C. DPV parameters were chosen as: pulse width: 0.05 s, pulse period: 0.2 s, wave amplitude: 0.10 V, and potential range: −1.2 V to +2.0 V.

2.5. Preparation of pharmaceutical infusion solution to analyze PAR

The developed electrode was used to determine PAR in an infusion solution containing a known amount of PAR as a real sample. The infusion solution sample was used directly without any pretreatment. Appropriate volumes of the sample solutions were added to 10 mL of supporting electrolyte in the

electrochemical cell to achieve the desired concentrations. Then, standard PAR solutions with known concentrations were added to this cell. Using the standard addition method, the concentration of PAR was determined. The concentration values of PAR were detected in the real sample with three repetitive measurements using DPV.

3. RESULTS AND DISCUSSION

3.1. Preparation of the 4P3T-GCE

The coating CVs of 4P3T on the GCE to develop 4P3T-GCE were obtained with 10 cycles. In the first cycle of CV, an anodic peak was observed at about +1.4 V potential with a small signal (**Figure 1**). The peak potential shifted to a negative direction in the second cycle. When the cycle numbers were increased, the anodic peak current increased in stages.

The shifting of peak potential and the increment of peak current indicated that the 4P3T film was formed on the GCE with increasing potential cycles [16-18].

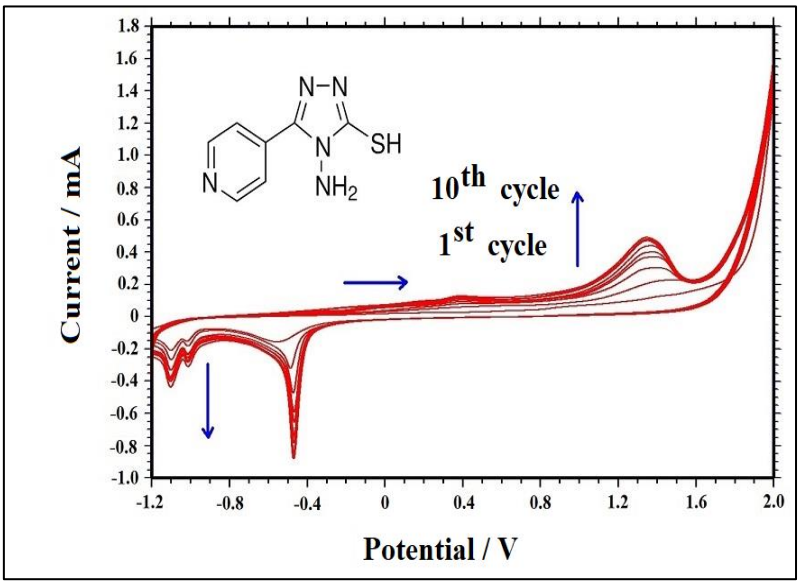

Figure 1. CV of the coating of 1.0 mM 4P3T molecule on the GCE surface in 0.1 M H_2SO_4 solution (vs Ag/AgCl electrode, ν = 100 mV s^{-1}).

3.2. The characterization of 4P3T-GCE by CV using redox species

$K_4[Fe(CN)_6]/K_3[Fe(CN)_6]$ and ferrocene redox species are frequently used to characterize the modified electrode surfaces [19]. **Figure 2(a)** and **Figure 2(b)** show the CVs of the redox species.

$K_4[Fe(CN)_6]/K_3[Fe(CN)_6]$ (5.0 mM) was prepared in 0.1 M KCl, while ferrocene (1.0 mM) was prepared in ACN solution

containing 0.1 M TBATFB. In order to determine the coating number, the electrode surfaces were coated for 5, 10, 15, 20, and 25 cycles. While the reduction and oxidation peak currents belonging to the redox species increased up to 10 cycles, they began to decrease thereafter. It was thought that this could be due to the peeling of the coating material from the surface after a specific CV cycle. As a result, it was decided that the most suitable coating number was 10 CV. The increase in peak currents of redox species on the modified surface, accompanied by an increase in conductivity, is due to the enhanced electron transfer kinetics.

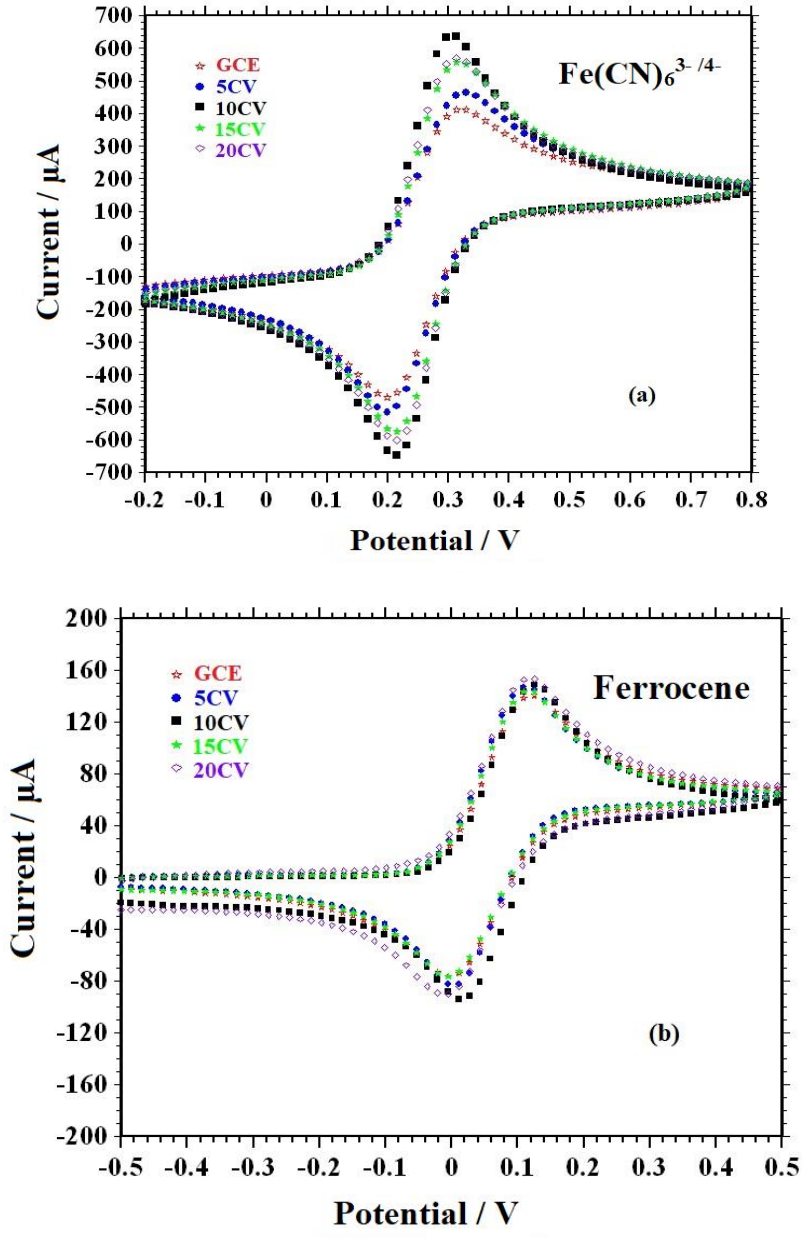

Figure 2. CVs (v= 100 mV s^{-1}) obtained for (a) $K_4[Fe(CN)_6]/K_3[Fe(CN)_6]$ (5.0 mM in 0.1 M KCl solution) (vs Ag/AgCl/KCl(sat.)) and (b) Ferrocene (1.0 mM in ACN containing 0.1 M

TBATFB) (vs Ag/Ag^{+}) on bare GCE and 4P3T-GCE prepared by coating with different (5, 10, 15, 20 and 25) cycles.

3.3. Electroactive surface areas of electrodes

The electroactive surface area of electrodes can be easily calculated using the CV technique. This process is done especially using a standard redox system ($[Fe(CN)_6]^{3-/4-}$). The process is performed based on the Randles–Sevcik equation [20]. The peak current, in reversible systems, measured by CV, is given below:

$$ipc = 2.69 \times 10^5 \, A \, n^{3/2} \, D^{1/2} \, C^{*} \, \nu^{1/2} \qquad (1)$$

According to the **Equation 1**, ν is the scan rate ($V\ s^{-1}$); C is the concentration of $K_3Fe(CN)_6$; A is the electroactive surface area (cm^2); D is the diffusion coefficient for $K_3Fe(CN)_6$ at 25°C ($D = 7.6 \times 10^{-6}\ cm^2\ s^{-1}$); ipc is the cathodic peak current of $K_3Fe(CN)_6$ and n is the number of electrons transferred for the redox reaction (n=1). The electroactive surface areas of uncovered and covered electrodes were calculated using the slope of the plot of ipc vs $\nu^{1/2}$. The various scan rates were selected between 10 mV s^{-1} and 200 mV s^{-1} for this study. It was found that the bare electrode's surface area was 0.054, while it was 0.081 cm^2 for the coated electrode.

A 1.5-fold increase in electroactive surface area was observed in 4P3T-GCE compared to bare GCE. This is evidence of coating the GCE surface with 4P3T, as the active area of the electrode surface increased significantly. Therefore, the conductivity was increased due to the high electroactive surface area of 4P3T-GCE, which facilitated the oxidation of PAR through rapid electron transfer.

3.4. The characterization with the EIS technique using an equivalent circuit model

EIS is an effective technique widely used to study the charge transfer kinetics at the electrode/solution interface and the electron transfer properties of modified electrode surfaces [21]. In **Figures 3(a)** and **3(b)**, Nyquist diagrams of the bare GCE and 4P3T-GCE in 5 mM $K_4[Fe(CN)_6]/K_3[Fe(CN)_6]$ solution containing 0.1 M KCl are presented. An alternating voltage was applied in the EIS measurements with an amplitude of 10 mV and a potential of 0.215 V (vs Ag/AgCl reference electrode), which corresponds to the formal potential of the $K_4[Fe(CN)_6]/K_3[Fe(CN)_6]$ system. The frequency range was applied between 0.01 Hz and 100 kHz. In the high-frequency

region, a semicircle was observed in the Nyquist diagrams, corresponding to the charge transfer process between the solution and electrode interface. In contrast, a curved linear section reflecting the diffusion-controlled process was observed in the low-frequency region. The Randles equivalent circuit model was used to fit and obtain EIS data using the CHI 660B software. This model includes the parameters Rs(electrolyte solution resistance), R_{ct} (charge transfer resistance), Qdl (double-layer capacitance), and W (Warburg impedance). As a result of comparing the bare GCE and 4P3T-GCE, it was observed that the surface modification had a significant effect on the impedance values. While the charge transfer resistance (R_{ct}) of the bare GCE was determined to be approximately 590 ohms, this value decreased to 119.3 ohms on the electrode surface modified with 4P3T.

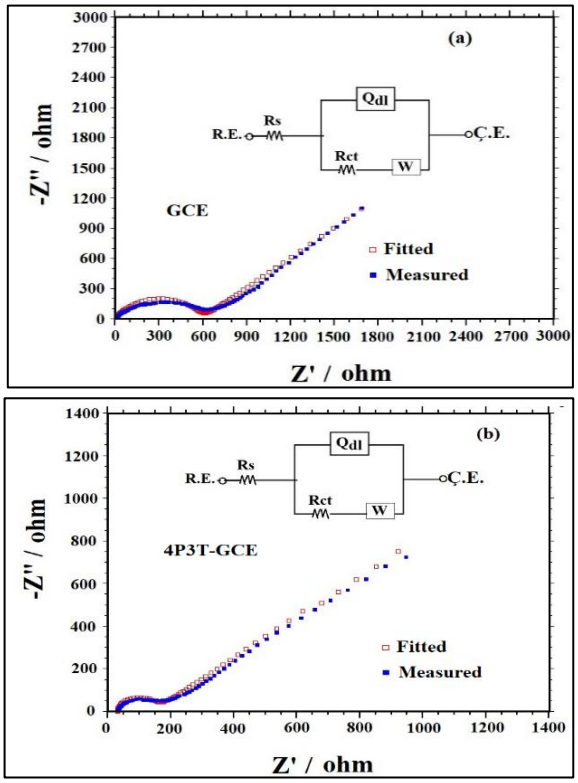

Figure 3. Nyquist plots, simulations, and equivalent circuits of (a) bare GCE and (b) 4P3T-GCE surfaces in a 0.1 M KCl solution containing 5 mM $K_4[Fe(CN)_6]/K_3[Fe(CN)_6]$, (c) comparative Nyquist plots of GCE and 4P3T-GCE (Potential = 0.215 V, Frequency range = 0.01 Hz-100 kHz, Amplitude = 10 mV).

The redox specie tests with CV were supported by the low charge transfer resistance, indicating that the electroactive area on the 4P3T-GCE electrode surface increases, and the electron transfer is accelerated accordingly. This decrease in R_{ct} confirms that the GCE surface is successfully coated with 4P3T. In addition, the high conductivity and large specific surface area of 4P3T-GCE enable the determination of PAR by oxidation.

In addition, the standard heterogeneous rate constant (k°) was calculated using the electrochemical analysis and the EIS results. The relation between the k° and R_{ct} was clarified using the equation of $R_{ct} = RT\times(n^2 F^2 Ak°[C])^{-1}$. Here, T and F are the temperature (298.15 K) and the Faraday constant (96485 C mol^{-1}), respectively. A is the surface area of the electrode (cm^2), and [C] is the redox specie's concentration (mol/cm^3). The k° values were calculated as 1.67×10^{-3} $cm\cdot s^{-1}$ for bare GCE and 5.51×10^{-3} $cm\cdot s^{-1}$ for 4P3T-GCE. This result showed that the electron transfer rate increased as the surface was modified.

3.5. The FT-IR measurement

The differences between solid 4P3T and 4P3T film, which is composed of the GCE, were determined by comparing their main IR bands. In IR spectra, the appearance of specific functional groups belonging to the solid material in the surface film, along with frequency shifts or the formation of different bonds between these groups, is evidence that the solid material is bonded to the surface. The FT-IR spectrum was recorded with 16 scans repeated between 4000 and 550 cm^{-1}, with a spectral resolution of 4 cm^{-1}, on the GCE surface using the IS5 ATR head. **Figures 4(a)** and **4(b)** show the FT-IR spectra of the 4P3T compound in the solid and the 4P3T film coated on GCE, respectively. These spectra reveal the chemical changes that occur with the attachment of the 4P3T molecule to the surface. To obtain the film spectrum that occurred with grafting 4P3T to GCE, the uncovered GCE spectrum was subtracted from the modified surface spectrum. In the spectrum of solid 4P3T (**Figure 4(a)**), the band observed at approximately 3269 cm^{-1} corresponds to the characteristic stretching vibrations of the $-NH_2$ group. On the other hand, when the spectrum of the 4P3T film coated on the GCE surface (**Figure 4(b)**) is examined, it is noteworthy that the characteristic vibrations of the $-NH_2$ group are not observed in the spectrum. This suggests that the $-NH_2$ group disappeared from the spectrum due to interaction with the surface or through another chemical transformation during film formation, and that binding to the surface may have occurred at this point. The bands observed between 3060 and 3158 cm^{-1} in the spectrum of the solid belong to aromatic C–H stretching [22]. These bands were observed at lower frequencies between 2956 and 2927 cm^{-1} in the surface film. The band observed in the solid spectrum at ~2857 cm^{-1}, thought to correspond to the

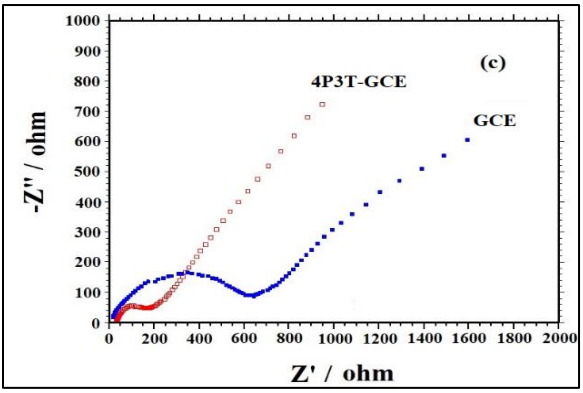

vibration of the S–H bond (ν S–H), shifted to a lower frequency in the film spectrum and was observed with a lower intensity at 2725 cm^{-1}. The bands corresponding to C=N, C–N, and N–H bending vibrations that appeared in the solid spectrum between 1605–1520 cm^{-1} were observed to be in the film spectrum between 1575–1518 cm^{-1}. In addition, a new band was detected in the film spectrum at ~1700–1600 cm^{-1}, the vibrations thought to belong to the –CO–NH group at ~1738 cm^{-1} [23]. This band is thought to be due to the formation of carbonyl groups on the GCE surface in the presence of H_2SO_4 during electrode coating; it was thought that the molecule formed a bond with -NH_2 in its structure and thus bonded to the surface. These observations confirm that the thiol and heteroaromatic rings in the structure of

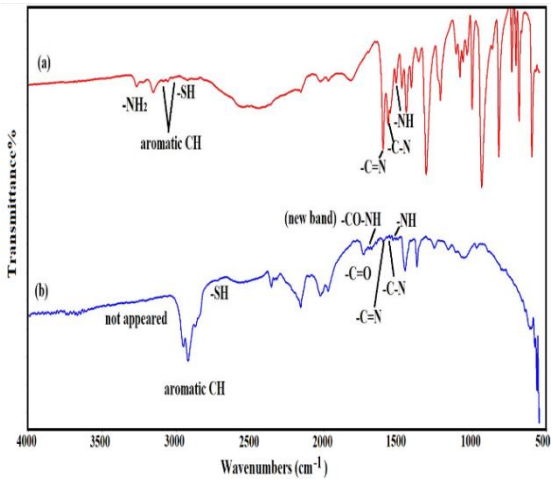

the 4P3T compound are also present in the surface film. In particular, the disappearance of the vibrations belonging to the -NH_2 group and the formation of a new amide (–CO–NH) band strongly support that the molecule has bonded to the surface. As a result, FT-IR analyses show that the surface modification of GCE with the 4P3T molecule has been successfully performed.

Figure 4. FT-IR spectra of a) Solid 4P3T and b) 4P3T film on GCE.

Aromatic C–H, C=N, and C–N bands are observed in both spectra; however, there was a decrease in the intensity of these bands and slight shifts in their wavenumbers in the film spectrum. This indicates changes in the environment of the molecule and possible chemical interactions after coating on the surface.

3.6. Analytical application of 4P3T-GCE

3.6.1. Investigation of the optimum conditions for PAR oxidation

In the electrochemical determination of PAR, the type of supporting electrolyte and its pH value, as the optimum conditions, play a crucial role in determining the intensity of the analytical signal and the peak potential [24].

In this study, the voltammetric responses obtained using DPV with different supporting electrolytes (pH 2.0 $HClO_4$, pH 2.0 H_2SO_4, pH 5.0 BR, pH 5.0 PBS, and pH 5.0 ABS at a 0.1 M concentration) were compared for PAR at the 4P3T-GCE (**Figure 5**). The fact that the concentration

and pH were at specific fixed values is for ease of comparison. It was found that the oxidation peak current value for 20 µM of PAR was high in the $HClO_4$ solution. However, since the peak shape was not very good and the current value obtained in this solution was close to the value obtained in PBS buffer, which is more commonly used in biological environments, PBS buffer was preferred as the most suitable supporting electrolyte. Since the peak current was higher on the 4P3T-GCE, and it occurred at a lower potential (it is oxidized more easily), PBS buffer was selected as a suitable supporting electrolyte to determine PAR more sensitively.

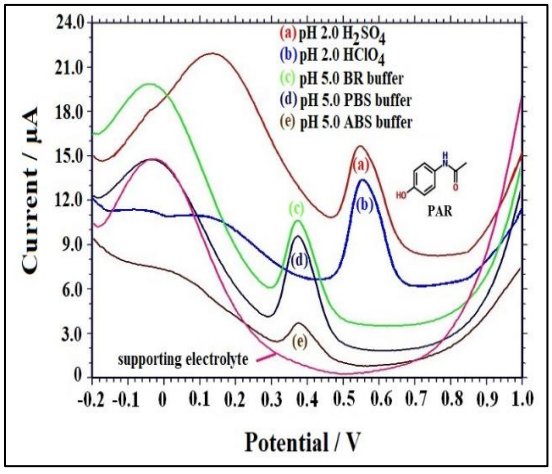

Figure 5. DPVs (vs Ag/AgCl/KCl (sat.) reference electrode) on the 4P3T-GCE in the presence of 20 µM PAR in different supporting electrolytes (0.1 M pH 5.0 PBS, ABS, and BR buffers, pH 2.0 H_2SO_4, and pH 2.0 $HClO_4$).

The pH value of the supporting electrolyte significantly affects the electrochemical behavior of PAR, too. Therefore, to evaluate the electrochemical oxidation properties of PAR, 4.0, 4.5, 5.0, 5.5, 6.0, and 8.0 pH values were examined in 0.1 M PBS buffer. The DPV results recorded at different pH values in solutions containing 20 µM PAR are presented in **Figure 6A**. As the pH increased, the oxidation peak potential shifted to more negative values. This confirms an electro-oxidation process in which proton incorporation occurs. In **Figure 6B**, DPVs of bare GCE and 4P3T-GCE were taken in the presence of 20 µM PAR at 0.1 M pH 4.5 PBS, and an approximately 20-fold increase in the PAR peak on the coated surface was observed compared to the bare surface. In other words, it was understood that the coated surface of GCE provided an advantage and that PAR was more easily oxidized on the modified electrode. It is shown from the ip-pH graph (**Figure 6C**) that the current increases from pH 4.0 to 4.5 and then decreases from 4.5 to 8.0. This shows that the optimum pH is 4.5. The most prominent peak is observed at pH 4.5, indicating that the electroanalytical signal of PAR is strongest at this pH, as both the highest current and the optimal potential value are obtained.

As given in the Ep-pH graph (**Figure 6D**), the shifting to lower positive potentials by 0.0529 V was observed on the oxidation peak potential of PAR (negative potentials) according to the equation Ep = −0.0529pH + 0.6398, R^2 = 0.991 for each unit increase in pH value. This is because protons play a role in the oxidation reaction of PAR. The m/n value was calculated according to the equation dEp/dpH = −0.059×(m/n), where n and m are the number of transferred electrons and the number of protons, respectively. The slope obtained from the plot of Ep vs pH (0.0529) was in agreement with 0.059 V, which is the theoretical value in the Nernst equation. Therefore, m/n is ~ 1, which means that the number of electrons and protons transferred is equal in the oxidation of PAR [25].

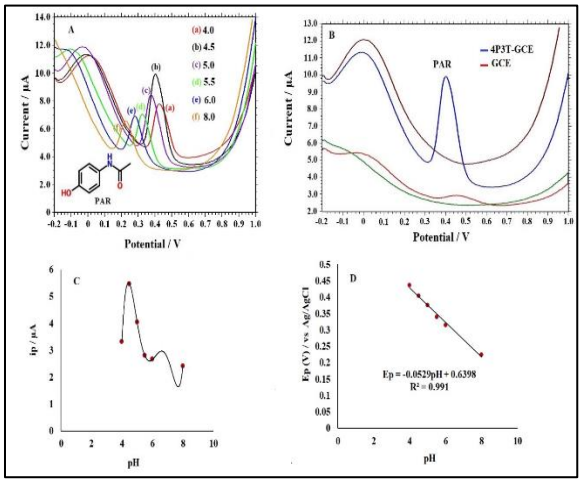

Figure 6. (A) The DPVs of 20 µM PAR in 0.1 M PBS buffer at different pH values on the 4P3T-GCE. (B) DPVs of 20 µM PAR in PBS buffer at pH 4.5 on the bare GCE and 4P3T-GCE. (C) ip-pH, and (D) Ep-pH plots on the 4P3T-GCE (vs Ag/AgCl/KCl(sat.)).

3.6.2. Effect of scan rate for PAR oxidation

Scan rate is an essential parameter in evaluating the electron transfer kinetics, reaction mechanism, and electrochemical activity of the modified electrode [26]. A scan rate study was conducted under optimal conditions to propose the electron transfer mechanism of PAR in relation to the oxidation reaction kinetics on the 4P3T-GCE surface. For this purpose, the CVs were taken at 25, 50, 75, 100, 200, 250, 300, 400, and 500 mV s^{-1} scan rates on the 4P3T-GCE surface in 0.1 M pH 4.5 PBS buffer containing 20 µM PAR (**Figure 7(a)**). It was seen that the anodic and cathodic peak currents (ipa and ipc) gradually increased when the scan rate (ν) increased. Whether the reduction-oxidation process on the electrode surface was controlled by diffusion or adsorption was found by plotting the logarithm of the scan rate (log ν) against the logarithm of the peak currents (log ipa and log ipc) (**Figure 7(b)**). Equations of the plot of this relationship were found as log ipa(µA)=0.7572logν−4.911 (R^2=0.9988) and log ipc(µA)=0.6918logν−5.493

(R^2=0.9979). The oxidation process of PAR on the 4P3T-GCE was both diffusion and adsorption-controlled because the slopes were found between 0.5 and 1.0 of the theoretical values [27]. It was seen in **Figure 7(c)** that as the scan rate increased, the anodic peak potentials were shifted to more positive values while the cathodic peak potentials of PAR were shifted to more negative values at 4P3T-GCE [28]. In other words, the increase occurred in the separation between the potentials of the anodic and cathodic peaks. According to Laviron's equation, the correlation of Ep-log ν is given below [29]:

$Epa(V)= 0.0545 \log\nu(V\ s^{-1}) + 0.524\ (R^2 =0.9493)$ (2)

$Epc(V)= -0.0431 \log\nu\ (V\ s^{-1}) + 0.3297\ (R^2 =0.9572)$ (3)

For the anodic and cathodic processes, the equations are given below:

$$Epa=E^{o'}+\frac{2.303\ RT}{zF(1-\alpha)}\log\frac{(1-\alpha)zF}{RTks}+\frac{2.303\ RT}{zF(1-\alpha)}\log\nu \quad (4)$$

$$Epc=E^{o'}-\frac{2.303\ RT}{zF\alpha}\log\frac{\alpha zF}{RTks}-\frac{2.303\ RT}{zF\alpha}\log\nu \quad (5)$$

Here, α is the electron transfer coefficient; ks is the rate constant of electron transfer at the interface; and z is the number of electrons. The meanings of the other symbols are given previously. The anode slope is 2.303RT/zF (1−α) and the cathode slope is -2.303RT/zFα. By substituting the slopes of the two lines (Epa-log ν and Epc-log ν) into **Equations 4** and **5**, α and z are calculated as 0.56 and 2.3~2, respectively.

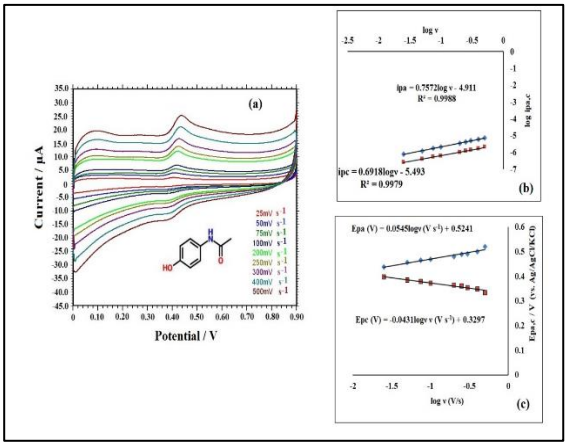

Figure 7. (a) CVs obtained for 20 µM PAR with 4P3T-GCE in 0.1 M pH 4.5 PBS buffer at different scan rates (25, 50, 75, 100, 200, 250, 300, 400, and 500 mV s^{-1}), (b) The plots of logip-logν, (c) The plots of Ep-logν.

The quasi-reversible behaviour in the electrochemical oxidation process of PAR was confirmed due to the increase in the peak separation (ΔEp) values as the scan rates increased. The electrochemical oxidation mechanism of PAR at 4P3T-GCE was suggested as seen in **Scheme 1** [30]. The result involved two electrons and two protons in the oxidation step of PAR.

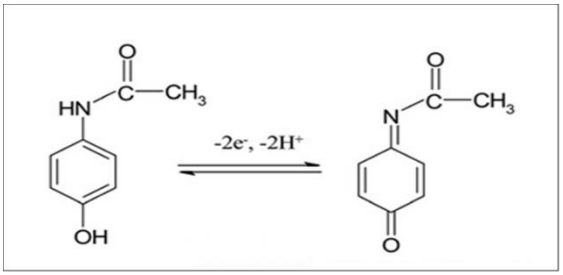

Scheme 1. Oxidation mechanism of PAR on the 4P3T-GCE surface.

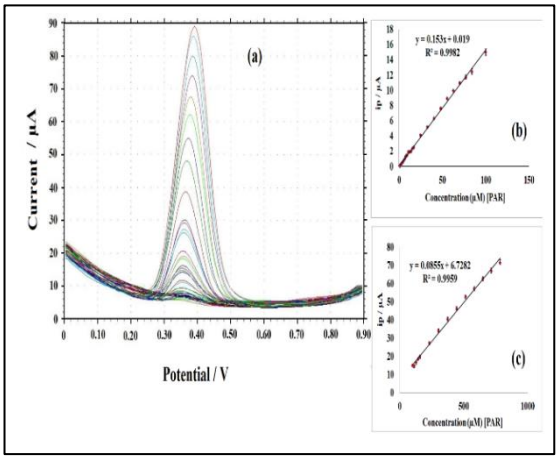

3.6.3. Calibration graph and analytical parameters of 4P3T-GCE for PAR

For PAR, the linear concentration range, LOD, and LOQ were determined using DPV in 0.1 M pH 4.5 PBS buffer on the 4P3T-GCE surface. For this purpose, DPVs obtained for different PAR concentrations are given in **Figure 8(a)**. The oxidation peak currents of PAR increased linearly in two different concentration ranges, 0.55–100 µM and 100–785 µM (**Figure 8(b, c)**).

The equations obtained from the calibration graphs are as follows: ipa[µA]= 0.0855C [µM] + 6.7282 (R^2= 0.9959) and ipa[µA]= 0.153C [µM] + 0.019 (R^2= 0.9982). The equations of 3s/m and 10s/m were used to find the LOD and LOQ values [31], respectively. Here, s is the standard deviation of the lowest concentration of PAR (n=7), and m is the slope of the first calibration graph. The LOD and LOQ values were calculated as 0.16 µM and 0.53 µM, respectively.

Figure 8. (a) DPVs of PAR at different concentrations in 0.1 M pH 4.5 PBS buffer obtained with 4P3T-GCE, (b) and (c) Calibration graphs (peak width = 0.05 s, amplitude = 0.1 V, sample time = 0.02 s, and peak period = 0.2 s).

The data revealed that 4P3T-GCE exhibited similar or significantly better analytical performance compared to other electrodes presented in **Table 1**. Firstly, the 4P3T-GCE was designed and used for the first time to determine sensitive PAR. Accordingly, our modified electrode offers the advantages of being quicker and easier to prepare than most electrodes, without requiring as much processing, and is also less expensive than some of them. Furthermore, compared to the studies in **Table 1**, the 4P3T-GCE has a lower LOD than most (32, 34, 35, and 37-40) with a wider linear operating range than most (32, 34, 35, and 37-39). The modified electrode provides more active sites, thus enhancing electrochemical performance thanks to the 4P3T molecule.

Modified Electrodes	Technique	Linear Range (µM)	LOD (µM)	Reference

CPE[a]/MgO	CV	10–100	6.2	[32]
SPCE[b] / CNFs[c]	DPAdsV	0.002–0.05 0.1–2.0	0.00054	[33]
poly(AHNSA)[d]/GCE	SWV	10–125	0.45	[34]
MWNT[e]/GCE	DPV	5–100	2.4	[35]
Sm_2O_3[f]@ZrO_2[g]/CNTs[h]/GCE	SWV	0.0037–2.2	0.00034	[36]
GPE[i]/cork	DPV	2.5–50	8.36	[37]
B:CNW[j]	DPV	0.032–32	0.281	[38]
Ni–Ti_3C_2@GNP[k]	CV, DPV	10–110	5.07	[39]
La@ZnO/AuNPs/GO[l]	DPV	0.5–1750	0.45	[40]
Protonated g-C_3N_4/CTS[m]-GCE	DPV	1.70–2020	0.15	[41]
4P3T-GCE	DPV	0.55–100 100–785	0.16	This study

Table 1. Comparison of the 4P3T-GCE with different electrodes for PAR determination.

[a]Carbon paste electrode, [b]Screen-printed carbon electrode, [c]Carbon nanofibers, [d]4-amino-3-hydroxy-naphthalene sulfonic acid, [e]Multilayer carbon nanotubes, [f]Samarium oxide, [g]Zirconium dioxide, [h]Carbon nanotubes, [i]Graphite paste electrode, [j]Boron-doped carbon nanowalls, [k]Nickel-doped Ti_3C_2 MXene-graphene nanoplatelets nanocomposite, [l]gold nanoparticles/graphene oxide, [m]Graphitic carbon nitride nanosheets chitosan.

3.6.4. Effects of interfering species, repeatability, and reproducibility

In electrochemical analyses, interfering species affect the analyte signal, causing erroneous measurement results. First, the voltammetric behaviors (peak potentials and currents) of known or suspected interfering substances in pure solution are examined separately. Then, a DPV voltammogram of a mixture of PAR and this interfering substance is obtained. If the PAR peak overlaps with the interfering substance peak, is very close, or causes a change in the PAR peak, interference is present. The change in the PAR signal is observed by adding increasing amounts of the interfering substance to a given PAR concentration. This indicates the impact of a given concentration of the interfering substance on the analytical signal.

The selectivity of the 4P3T-GCE electrode was evaluated under optimized conditions. So, the effects of several interfering species on the determination of PAR were tested using the DPV technique. These species were selected from the group of substances commonly found with PAR. It was observed that the peak current and potential of PAR (20 µM) did not change significantly under optimal conditions (signal change ≤6%) up to the concentrations indicated for the species in **Table 2**. Above these concentrations, a decrease in the peak current and potential shifts of PAR were observed. Therefore, it was concluded that in the presence of different species, even at high concentrations used in Table 2, 4P3T-GCE had a good anti-interference ability.

Table 2. Interference effects of some species in a 0.1 M pH 4.5 PBS buffer containing 20 µM PAR with the 4P3T-GCE.

Interfering Species	Concentration* (µM)	Species/Analyte Ratio
K^+	2000	100/1
Na^+	2000	100/1
Zn^{2+}	2000	100/1
Cl^-	2000	100/1
SO_4^{2-}	1000	50/1
Glucose	1000	50/1
p-Aminophenol	600	30/1

*Maximum concentration of species tested with the deviations below 6%.

For repeatability, 10 consecutive DPVs were taken in the presence of 20 µM PAR in 0.1 M pH 4.5 phosphate buffer using the same modified electrode. This study demonstrated acceptable repeatability of 4P3T-GCE with a relative standard deviation (RSD%) of 3.8%.

In order to study the reproducibility for PAR determination at optimum conditions, five 4P3T-GCEs were prepared independently, and the RSD% value at peak currents of these electrodes was calculated as 5.4%.

3.6.5. Real sample analysis

The prepared electrode was applied to the determination of PAR by the standard addition method in an infusion solution with a PAR concentration of 10 mg/mL. To eliminate matrix effects, the infusion solution sample was added directly to the cell without pretreatment. To determine the spike PAR concentration, known amounts of PAR (standard additions) were successively added to the existing sample solution using the DPV technique. The results from the measurements are given in **Table 3**. The values of RSD% were 3.2%, 2.8%, and 2.4%, and the values of recovery were 104%, 103%, and 101%, respectively. These results showed that it is possible to determine PAR in the real sample at the 4P3T-GCE with good accuracy and sensitivity.

Table 3. Results of analysis of PAR in infusion solution as a real sample using 4P3T-GCE.

Infusion Solution	Known PAR (µM)	Found PAR (µM)	Relative Error%	RSD%	Recovery%

Sample					
1	5.0	5.2±0.3*	+3.6	3.2	104
2	10.0	10.3±0.5	+3.1	2.8	103
3	25.0	25.2±0.6	+0.8	2.4	101

*90% confidence interval for three measurements.

4. Conclusions

This study presents an electrochemically modified electrode (4P3T-GCE) for PAR determination. The surfaces of the electrodes were characterized using EIS, CV, and FTIR techniques to compare the surface features of each other. The modified GCE offers significant analytical advantages over other electrodes in the literature. These advantages make this developed modified electrode stand out, particularly in terms of its ease and rapid preparation, high sensitivity, wide linear concentration range, and cost-effectiveness. One of the most significant advantages of our electrode is its low limit of detection for PAR determination under optimal operating conditions (LOD: 0.16 µM) with good repeatability and reproducibility. This value is quite competitive with, and even lower than, many PAR determination methods reported in the literature. A low LOD is critical for the reliable and accurate determination of low concentrations of PAR, particularly in biological fluids, environmental samples, or pharmaceutical formulations. While many PAR determination methods in the literature using various electrodes generally offer narrower or single linear ranges, the two-stage, wide linear working range found in this study (0.55-100 µM (for low and medium concentrations) and 100-785 µM (for higher concentrations) offers the flexibility to adapt to various PAR concentrations in different sample matrices easily. This simplifies sample preparation processes and increases analytical efficiency.

In the present study, the surface area of the 4P3T-GCE increased almost 1.5-fold compared to that of bare GCE. The 4P3T film formed on the GCE surface increased the active electrode surface area, electrical conductivity, and electron transfer rate, facilitating the electrochemical oxidation of PAR.

Using the DPV technique with the 4P3T-GCE electrode, PAR was determined at different concentrations in an infusion solution sample using the standard addition method with good recovery percentages

and low error values, demonstrating the high accuracy of this method in pharmaceutical samples.

5. Ethics approval and consent to participate

This study does not need an Ethics report.

6. Consent for publication

The Authors give consent for publication.

7. Availability of data and materials

All data and materials of the paper are available to the public.

8. Authors' contributions

Demet UZUN: Methodology, experimental, conceptualization, writing, supervisor, Alev YILDIRIM: Investigation, experimental.

Disclosure statement

No potential conflict of interest was reported by the author(s).

REFERENCES

1. Bakht K, Alrowaily AW, Alotaibi BM, et al (2025) Fabrication of $CoFe_2O_4$/PANI nanocomposite modified glassy carbon electrode for the electrochemical determination of paracetamol. Journal of the Indian Chemical Society 102: 102080. https://doi.org/10.1016/j.jics.2025.102080

2. Shih Y-J, Lin S-K, Wu Z-L, Chen W-H. (2024) Cobalt and zinc imidazolate encapsulated in reduced graphene oxide and the derived nitrogen-enriched carbon frameworks (CoNC@rGO) for electrochemically sensing acetaminophen (APAP). Chemical Engineering Journal 481: 148437. https://doi.org/10.1016/j.cej.2023.148437

3. Van der Marel CD, Anderson BJ, van Lingen RA, et al (2003) Paracetamol and metabolite pharmacokinetics in infants. European Journal of Clinical Pharmacology 59(3): 243–251. https://doi.org/10.1007/s00228-003-0608-0

4. Kassa A, Amare M (2019) Electrochemical determination of paracetamol, rutin and sulfonamide in pharmaceutical formulations by using glassy carbon electrode – A review. Cogent Chemistry 5(1): 1681607. https://doi.org/10.1080/23312009.2019.1681607

5. Wang Y, Yang G, Chu M, et al (2024) Construction of MOF-74-derived CuFe/C alloy highly dispersed on ultrathin single layered reduced graphene for electrochemical determination of paracetamol. Journal of Alloys and Compounds 998: 174989. https://doi.org/10.1016/j.jallcom.2024.174989

6. Sadok I,. Tyszczuk-Rotko K (2015) New, simple and sensitive voltammetric procedure for determination of paracetamol in pharmaceutical formulations. Insights in Analytical Electrochemistry 1: 1–8. https://doi.org/10.4172/2470-9867.100001

7. Teker T, Bağdiken FN, Aslanoglu M (2025) Ultrasonic-assisted development of a high-sensitivity voltammetric sensor based on graphene nanoplatelets and hafnium oxide nanomaterials for paracetamol detection. Microchemical Journal 213: 113862. https://doi.org/10.1016/j.microc.2025.113862

8. Arancibia V, Penagos-Llanos J, Nagles E, et al (2019) Development of a microcomposite with single-walled carbon nanotubes and Nd_2O_3 for determination of paracetamol in pharmaceutical dosage by adsorptive voltammetry. Journal of Pharmaceutical Analysis 9: 62–69. https://doi.org/10.1016/j.jpha.2018.11.005

9. Cabas Rodriguez JA, Bonetto A, Alaniz RD, et al (2024) Electrochemical sensor based on a glassy carbon electrode modified with a 3D carbon nanoporous composite for the detection of paracetamol in pharmaceutical samples. Journal of Electroanalytical Chemistry 973: 118689. https://doi.org/10.1016/j.jelechem.2024.118689

10. Doğan B, Elik A, Altunay N (2020). Determination of paracetamol in synthetic urea and pharmaceutical samples by shaker-assisted deep eutectic solvent microextraction and spectrophotometry. Microchemical Journal 154: 104645 https://doi.org/10.1016/j.microc.2020.104645

11. Easwaramoorthy D, Yu Y-C, Huang H-J (2001) Chemiluminescence detection of paracetamol by a luminol–permanganate based reaction. Analytica Chimica Acta 439: 95–100. https://doi.org/10.1016/S0003-2670(01)00968-0

12. Migowska N, Caban M, Stepnowski P, Kumirska J (2012) Simultaneous analysis of nonsteroidal anti-inflammatory drugs and estrogenic hormones in water and wastewater samples using gas chromatography–mass spectrometry and gas chromatography with electron capture detection. Science of the Total Environment 441: 77–88. https://doi.org/10.1016/j.scitotenv.2012.09.043

13. Kannan K, Ayyadurai N, Sevvel P, Ranganathan TV (2017) A highly selective and simultaneous determination of paracetamol and dopamine using poly-4-amino-6-hydroxy-2-mercaptopyrimidine (Poly-AHMP) film modified glassy carbon electrode. Journal of Electroanalytical Chemistry 791:8–16. https://doi.org/10.1016/j.jelechem.2017.03.002

14. Zhao S, Bai W, Yuan H, et al (2006) Detection of paracetamol by capillary electrophoresis with chemiluminescence detection. Analytica Chimica Acta 559: 195–199 https://doi:10.1016/j.aca.2005.11.071

15. Biswas S, Chakraborty D, Das R, et al (2015) A simple synthesis of nitrogen doped porous graphitic carbon: Electrochemical determination of paracetamol in presence of ascorbic acid and p-aminophenol. Analytica Chimica Acta 890: 98–107. https://doi.org/10.1016/j.aca.2015.07.045

16. Tabanlıgil Calam T (2025) A new modified electrode for the simultaneous determination of hydroquinone and catechol in environmental samples and optimization of voltammetric parameters by response surface methodology. Journal of Environmental Chemical Engineering 13: 118155. https://doi.org/10.1016/j.jece.2025.118155

17. Girum W, Kassa A (2025) Green voltammetric strategy for sensitive determination of paracetamol in pharmaceuticals and serum using alizarin red S-modified glassy carbon electrodes. Sensing and Bio-Sensing Research 48: 100792. https://doi.org/10.1016/j.sbsr.2025.100792

18. Kannan A, Sevvel R (2017) A highly selective and simultaneous determination of paracetamol and dopamine using poly-4-amino-6-hydroxy-2-mercaptopyrimidine (Poly-AHMP) film modified glassy carbon electrode. Journal of Electroanalytical Chemistry 791: 8–16. http://dx.doi.org/10.1016/j.jelechem.2017.03.002

19. Bayram E, Akyilmaz E (2016) Development of a new microbial biosensor based on conductive polymer/multiwalled carbon nanotube and its application to paracetamol determination. Sensors and Actuators B 233: 409–418. http://dx.doi.org/10.1016/j.snb.2016.04.029

20. Bard AJ, Faulkner LR (2001) Electrochemical methods: Fundamentals and applications. New York: John Wiley and Sons, 304–309.

21. Zhong W, Yang J, Yansha G, et al (2021) Electrochemical determination of paracetamol using MXene/single-walled carbon nanohorns composite as sensor. International Journal of Electrochemical Science 16: 211150. https://doi.org/10.20964/2021.11.39

22. Soares LA, da Silveira TFS, Silvestrini DR, et al (2013) A new hybrid polyhedral cubic silsesquioxane chemically modified with 4-amino-5-(4-pyridyl)-4H-1,2,4-triazole-3-thiol (APTT) and copper hexacyanoferrate(III) for voltammetric determination of nitrite. International Journal of Electrochemical Science 8: 4654–4669.

23. Nkune NW, Kruger CA, Abrahamse H (2022) Synthesis of a novel nanobioconjugate for targeted photodynamic therapy of colon cancer enhanced with cannabidiol. Oncotarget 13: 156–172. https://doi.org/ 10.18632/oncotarget.28171

24. Niaz A, Arain MB, Soylak M (2025) Highly sensitive and efficient voltammetric method for the determination of 4-aminophenol in paracetamol tablet and urine samples using screen printed carbon electrode modified with humic acid functionalized iron oxide nanoparticles. Inorganic Chemistry Communications 174: 114005. https://doi.org/10.1016/j.inoche.2025.114005

25. Stoytcheva M, Zlatev R, Velkova Z, et al (2023) The validity of using bare graphite electrode for the voltammetric determination of paracetamol and caffeine. International Journal of Electrochemical Science 18: 100120. https://doi.org/10.1016/j.ijoes.2023.100120

26. Demir E, Göktug Ö, İnam R, et al (2021) Development and characterization of iron (III) phthalocyanine modified carbon nanotube paste electrodes and application for determination of fluometuron herbicide as an electrochemical sensor. Journal of Electroanalytical Chemistry 895: 115389. https://doi.org/10.1016/j.jelechem.2021.115389

27. Tabanlıgil Calam T (2021) A novel, efficient and sensitive method for the simultaneous determination of riboflavin (vitamin B2) and pyridoxine hydrochloride (vitamin B6) in food and pharmacological samples using an electrochemical sensor based on 4,4′ -diamino benzophenone. Microchemical Journal 169: 106557. https://doi.org/10.1016/j.microc.2021.106557

28. Hanabaratti RM, Tuwar SM, Nandibewoor ST, et al (2020) Fabrication and characterization of zinc oxide nanoparticles modified glassy carbon electrode for sensitive determination of paracetamol. Chemical Data Collections 30: 100540 https://doi.org/10.1016/j.cdc.2020.100540

29. Laviron EJJ (1979) General expression of the linear potential sweep voltammogram in the case of diffusionless electrochemical systems. Journal of Electroanalytical Chemistry and Interfacial Electrochemistry 101: 19–28.

30. Zhang X, Kang S, Chen L-W (2025) MOF-derived N-doped porous carbon anchoring atomically-dispersed Fe for electrochemical sensing of paracetamol. Microchemical Journal 212: 113394. https://doi.org/10.1016/j.microc.2025.113394

31. Ansen Z, Tabanlıgil Calam T (2025) Optimization of voltammetric parameters and sensitive determination of hazardous 2-nitrophenol in environmental media using a modified glassy carbon electrode based on 2-amino nicotinamide. Journal of Water Process Engineering 76: 108165. https://doi.org/10.1016/j.jwpe.2025.108165

32. Manjunatha KG, Kumara Swamy BE, Madhuchandra HD, et al (2021) Synthesis and characterization of MgO nanoparticle and their surfactant modified carbon paste electrode sensing for paracetamol. Sensors International 2: 100127. https://doi.org/10.1016/j.sintl.2021.100127

33. Sasal A, Tyszczuk-Rotko K, Chojecki M, et al (2020) Direct determination of paracetamol in environmental samples using screen-printed carbon/carbon nanofibers sensor – Experimental and theoretical studies. Electroanalysis 32(7): 1618–1628. https://doi.org/10.1002/elan.202000039

34. Tefera M, Geto A, Tessema M, et al (2016) Simultaneous determination of caffeine and paracetamol by square wave voltammetry at poly(4-amino-3-hydroxynaphthalene sulfonic acid)-modified glassy carbon electrode. Food Chemistry, 210, 156–162. https://doi.org/10.1016/j.foodchem.2016.04.106

35. Wan Q, Wang X, Yu F, et al (2009) Effects of capacitance and resistance of MWNT-film coated electrodes on voltammetric detection of acetaminophen. Journal of Applied Electrochemistry 39(7): 1145–1151. https://doi.org/10.1007/s10800-008-9773-2

36. Teker T, Aslanoglu M (2020) Sensitive and selective determination of paracetamol using a composite of carbon nanotubes and nanoparticles of samarium oxide and zirconium oxide. Microchemical Journal 158: 105234. https://doi.org/10.1016/j.microc.2020.105234

37. Monteiro MKS, Santos ECMM, Silva DR, et al (2020) Simultaneous determination of paracetamol and caffeine in pharmaceutical formulations and synthetic urine using cork-modified graphite electrodes. Journal of Solid State Electrochemistry 24: 1789–1800. https://doi.org/10.1007/s10008-020-04722-y

38. Niedziałkowski P, Cebula Z, Malinowska N, et al (2019) Comparison of the paracetamol electrochemical determination using borondoped diamond electrode and boron-doped carbon nanowalls. Biosensors and Bioelectronics 126: 308–314. https://doi.org/10.1016/j.bios.2018.10.063

39. Bhardwaj V, Awasthi A, Pathania AR, et al (2026) Ni-doped Ti3C2 MXene@graphene for electrochemical detection of paracetamol. Materials Chemistry and Physics 349: 131774. https://doi.org/10.1016/j.matchemphys.2025.131774

40. Shafaq H, Anjum S, Muntaha ST, et al (2025) Design of La@ZnO/AuNPs/GO nanocomposites as an electrochemical sensor for acetaminophen detection. Sensing and Bio-Sensing Research 50: 100929. https://doi.org/10.1016/j.sbsr.2025.100929

41. Achache M, García-Guzman´ JJ, Seddik NB, et al (2025) Voltammetric detection of paracetamol using a novel Sonogel-Carbon material modified with monocalcium phosphate: An experimental and theoretical approach. Diamond & Related Materials 154: 112141. https://doi.org/10.1016/j.diamond.2025.112141